Check for updates

DR. PATRICIA DE NADAI (Orcid ID : 0000-0001-6084-7447)
DR. ANNE TSICOPOULOS (Orcid ID : 0000-0002-1579-2763)

Article type : Letter to the Editor

LETTER TO THE EDITOR

Direct activation of the aryl hydrocarbon receptor by dog allergen participates in airway neutrophilic inflammation

To the Editor,

Asthma is a chronic disorder, characterized by airway hyperresponsiveness (AHR), variable bronchial remodelling, and by an inflammatory process leading to fluctuating recruitment of eosinophils and neutrophils. Among asthma patients, up to 10% exhibit severe asthma and display type 2 (T2)- low and -high phenotypes. Besides T2 cytokines, Th17-type cytokines are also a driver of severe asthma pathophysiology, through induction of airway neutrophil infiltration, AHR, bronchial remodelling, and corticosteroid resistance. One determinant of Th17-type cytokine production is the transcription factor aryl hydrocarbon receptor (Ahr). This receptor is activated by small molecules provided by the diet, microorganisms, metabolism and by pollutants. In T cells, Ahr controls IL-17 and IL-22 transcription, but can also induce CD4 T cells with a regulatory phenotype. Depending on the Ahr ligand used, opposite results have been published in allergic airway inflammation (AAI) reporting anti- and pro- inflammatory effects[1]. The aim of this study was to develop a model of neutrophilic AAI exhibiting Th17-type features to evaluate the effect of Ahr blockade.

A mouse model of dog allergen-induced AAI was developed (Figure S1A), an allergen associated with more severe asthma in humans[2]. Dog allergen-challenged mice exhibited all the cardinal features of AAI, including increases in broncho alveolar lavage (BAL) total cell numbers, in relation with a high number of neutrophils and to a lesser extent with eosinophil and lymphocyte elevations (Figures 1A and S1B), raised total and dog allergen-specific serum IgE (Figure 1B), and elevated AHR (Figure 1C). The cytokine profile of lung extracts showed that although BAL eosinophil counts were low in this model, Th2-type cytokines and chemokine *Il-4*, *Il-13*, IL-33 and

This article has been accepted for publication and undergone full peer review but has not been through the copyediting, typesetting, pagination and proofreading process, which may lead to differences between this version and the Version of Record. Please cite this article as doi: 10.1111/ALL.14740

This article is protected by copyright. All rights reserved

Accepted Article

CCL17 were upregulated in the lungs of dog allergen-challenged mice, as were IL-17, IL-22 and neutrophil attracting CXCL1 and CXCL2, but not IFN-γ (Figures 1D and S1C). Cells known to produce IL-17 and IL-22 were analysed by flow cytometry (Figure S2). In dog allergen-stimulated groups, $CD4^+$ T cells, γδT cells and lymphoid tissue inducer cells (LTi), a subset of ILC3, appeared to be the major cell subsets expressing both IL-17 and IL-22 (Figure 1E). Other analysed cells did not significantly contribute to this cytokine production after allergen challenge (Figure S1D). These data are in agreement with other studies in lung infection models.[3] These pro Th17 effects may relate to dog allergen composition, which includes lipocalin Can f 1, able to bind the mannose and DC-SIGN receptors that promote Th17 responses to fungal infections. Histological analysis of lung sections from dog allergen- compared with PBS- challenged mice showed an increase in Hematoxylin & Eosin stained cell infiltrates, in Periodic Acid-Schiff stained mucus and in peri-bronchial collagen depots as assessed by Masson's trichrome staining, Picrosirius red staining, and two-photon microscopy, as well as thicker bronchial smooth muscle cell (SMC) layer assessed by anti α-smooth muscle actin (α-SMA) staining, and the presence of ectopic follicles resembling induced bronchus associated lymphoid tissue (iBALT) (Figures 1F and S1E). iBALT are tertiary lymphoid organs composed of B, T cells, germinal centers with follicular dendritic cells (FDC). $CD21^+$FDC, $B220^+$B cells, and $CD3^+$T cells, were assessed by immunohistochemistry and found in the peri-bronchial ectopic follicles (Figure 1G). Total IgA and dog allergen-specific IgG1 were strongly increased in BAL from the dog allergen-challenged but not from the control group (Figure 1G). Although the presence of BALT has been observed in bronchial biopsies from asthmatic patients, their relationship with the severity of asthma and their cause remain unclear. Pathogen-derived LPS is able to favour the induction of iBALT, however, much higher doses (1 to 10 μg)[3] than those present in our extracts (50 ng cumulative dose) are necessary. In lung infection models, IL-17 deficiency may[3] or may not[4] alter iBALT development depending on the infectious agent used. Finally, IL-22 has been described to favour formation of tertiary lymphoid organs in virus-infected salivary glands in mice.[5] Whether IL-17 and/or IL-22 initiate iBALT formation in our AAI model will need further investigations.

As Ahr controls the expression of IL-17 and IL-22, we wondered if dog allergen may contain an Ahr ligand. In reporter cell lines for the human and murine Ahr, dog allergen and in particular Can f 2, but neither house dust mite nor LPS induced a dose dependent luciferase reporter activity (Figure 2A and S3A). These data suggest that Ahr may participate in the features of dog allergen-induced AAI. The effect of Ahr blockade was evaluated using an antagonist as a curative treatment. The Ahr antagonist CH-223191 was administered through the diet during the challenge phase. In allergic mice, it reduced BAL total cell and neutrophil recruitment and AHR, but neither BAL eosinophils and lymphocytes nor the humoral response compared with non-

This article is protected by copyright. All rights reserved

treated mice (Figure 2B and S3B). Dog allergen-induced IL-22 production but not the others cytokines including IL-17, was down regulated by Ahr antagonist treatment (Figure 2C). Attenuated IL-22 production following Ahr antagonism may explain the decreased neutrophil infiltration and AHR, through IL-22 capacity to recruit neutrophils,[6] which are involved in AHR induction[7]. Histological analysis of lung sections from treated allergic mice evidenced no changes in the inflammation score, or collagen deposition, but showed a decrease in mucus production and in the thickness of SMC (Figure 2D and S3C). Decreased mucus production may be attributed either to direct inhibition of Ahr that has been involved in mucin production, or to decreased IL-22 that may also participate in the decreased hyperplasia of airway SMC.[8] Interestingly, the number of iBALT was increased in Ahr antagonist treated allergic mice (Figure S3D), as were BAL allergen-specific IgG1 antibodies (Figure 2E), FDC and B cell numbers, whereas the number of $CD3^+$, $Foxp3^+$ regulatory T cells and BAL total IgA antibodies (Figures 2E, 2F and S3D) were not modified. As IgG1 antibodies bind the inhibitory FcγRIIB receptor able to suppress AAI,[9] this induction might be beneficial in our model. This study provides a novel preclinical model of asthma to assess new therapeutic strategies for the Th17-type endotype. Altogether these results indicate that the Ahr pathway may provide a therapeutic approach for neutrophilic asthma, not targeted by currently available biotherapies.

REFERENCES

1. Poulain-Godefroy O, Boute M, Carrard J, et al. The Aryl Hydrocarbon Receptor in Asthma: Friend or Foe? *Int J Mol Sci*. 2020;21:8797.
2. Perzanowski MS, Ronmark E, James HR, et al. Relevance of specific IgE antibody titer to the prevalence, severity, and persistence of asthma among 19-year-olds in northern Sweden. *J Allergy Clin Immunol*. 2016;138:1582-90.
3. Rangel-Moreno J, Carragher DM, de la Luz Garcia-Hernandez M, et al. The development of inducible bronchus-associated lymphoid tissue depends on IL-17. *Nat Immunol*. 2011;12:639-46.
4. Fleige H, Haas JD, Stahl FR, et al. Induction of BALT in the absence of IL-17. *Nat Immunol*. 2011;13:1; author reply 2.
5. Barone F, Nayar S, Campos J, et al. IL-22 regulates lymphoid chemokine production and assembly of tertiary lymphoid organs. *Proc Natl Acad Sci U S A*. 2015;112:11024-9.
6. Stacey MA, Marsden M, Pham NT, et al. Neutrophils recruited by IL-22 in peripheral tissues function as TRAIL-dependent antiviral effectors against MCMV. *Cell Host Microbe*. 2014;15:471-83.

This article is protected by copyright. All rights reserved

7. Ekstedt S, Safholm J, Georen SK, et al. Dividing neutrophils in subsets reveals a significant role for activated neutrophils in the development of airway hyperreactivity. *Clin Exp Allergy*. 2019;49:285-91.
8. Chang Y, Al-Alwan L, Risse PA, et al. Th17-associated cytokines promote human airway smooth muscle cell proliferation. *FASEB J*. 2012;26:5152-60.
9. Dharajiya N, Vaidya SV, Murai H, et al. FcgammaRIIb inhibits allergic lung inflammation in a murine model of allergic asthma. *PLoS One*. 2010;5:e9337.

ACKNOWLEDGEMENTS

We acknowledge the generous support from the NIAID (National Institutes of Health) Tetramer Facility (Emory University, Atlanta, GA) for supplying CD1d tetramers and Dr. W. Ouyang (Genentech, San Francisco, CA) for the anti-IL-22 Ab (clone 3F11). The murine AhR reporter cell line (H1L7.5c3 mouse hepatoma) was kindly provided by Michael Denison (Davis University, CA). This work was supported by a grant from Santelys, and by a fellowship to MB by Fonds de Recherche en Santé Respiratoire.

CONFLICT OF INTEREST

Dr. Chenivesse reports grants from AstraZeneca, Santélys, personal fees from ALK-Abello, AstraZeneca, Boehringer Ingelheim, GlaxoSmithKlein, Novartis, Roche, Sanofi, and TEVA. , non-financial support from ALK-Abello, AstraZeneca, Boehringer Ingelheim, Chiesi, GlaxoSmithKlein, MEDA Pharma, Medexact, Novartis, Pierre Fabre, Pfizer, outside the submitted work; Dr. Tsicopoulos reports grants from Santelys, during the conduct of the study; non-financial support from Astra Zeneca, personal fees from ALK-Abello, outside the submitted work. All others authors declare that they have no relevant conflict of interest.

Mélodie Bouté[1], Saliha Ait Yahia[1], Julie Nanou[1], Daniel Alvarez-Simon[1], Camille Audousset[1,] Han Vorng[1], Joanne Balsamelli[1], Fan Ying[1], Philippe Marquillies[1], Elisabeth Werkmeister[1], Patricia de Nadai[1], Cécile Chenivesse[1*], Anne Tsicopoulos[1*]

[1]Univ. Lille, CNRS, Inserm, CHU Lille, Institut Pasteur de Lille, U1019-UMR9017-CIIL-Centre d'Infection et d'Immunité de Lille, Lille, France

* These authors equally contributed to the work.

Correspondence:

Anne Tsicopoulos, Center for Infection and Immunity of Lille,

This article is protected by copyright. All rights reserved

U1019 Pulmonary Immunity
Institut Pasteur de Lille, 1 rue du Professeur Calmette
59019 Lille Cedex, France
E-mail: anne.tsicopoulos@pasteur-lille.fr

Author contributions

MB, SAY, JN, HV, DAS, CA, HV, JB, FY, PM, EW, PdN, CC and AT designed and performed experiments; AT drafted the paper, AT, MB, SAY, CC, CA, DAS and PdN analysed and wrote the manuscript. All authors read and approved the manuscript.

Legends to figures

Figure 1. Dog allergen extract induces neutrophilic airway inflammation, AHR, bronchial remodelling and iBALT formation

A, BAL absolute number of cells. **B**, Total IgE and specific IgE (titers) in sera. **C,** Airway hyperresponsiveness. **D**, Levels of cytokines in lung extracts and BAL (IL-22). **E,** Numbers of IL-17$^+$ and IL-22$^+$ cells in the lungs. LTi: lymphoid tissue inducer cells **F**, Representative photographs and quantification of stained lung sections for inflammation using H&E (black stars), mucus using PAS (pink colour), collagen using Masson's trichrome (blue/green staining), SMC using α-SMA antibody (positive cells are stained in red), BM: basement membrane. Black arrows show staining of interest (mucus, collagen and SMC). V: vessel, Br: bronchus. **G**, Representative photographs and quantification of iBALT: numbers per iBALT of FDC, B cells T cells. Positive cells are stained in red. Black arrows show staining of interest**.** Numbers of iBALT, BAL total IgA and dog allergen-specific IgG1. Scale bars: 100 µm. Data are presented as mean ± SEM of n mice per group (n=14-32 for A, B and C, n=8-20 for D, n=6-15 for E, and n=4-7 for histology, n=13-22 for BAL in G). *p<0.05, **p<0.01, ***p<0.001, versus PBS. Mann Whitney test for all and two-way ANOVA for AHR.

Figure 2. Ahr antagonist alleviates AHR, BAL neutrophil infiltration and lung IL-22 production and increases BALT formation.

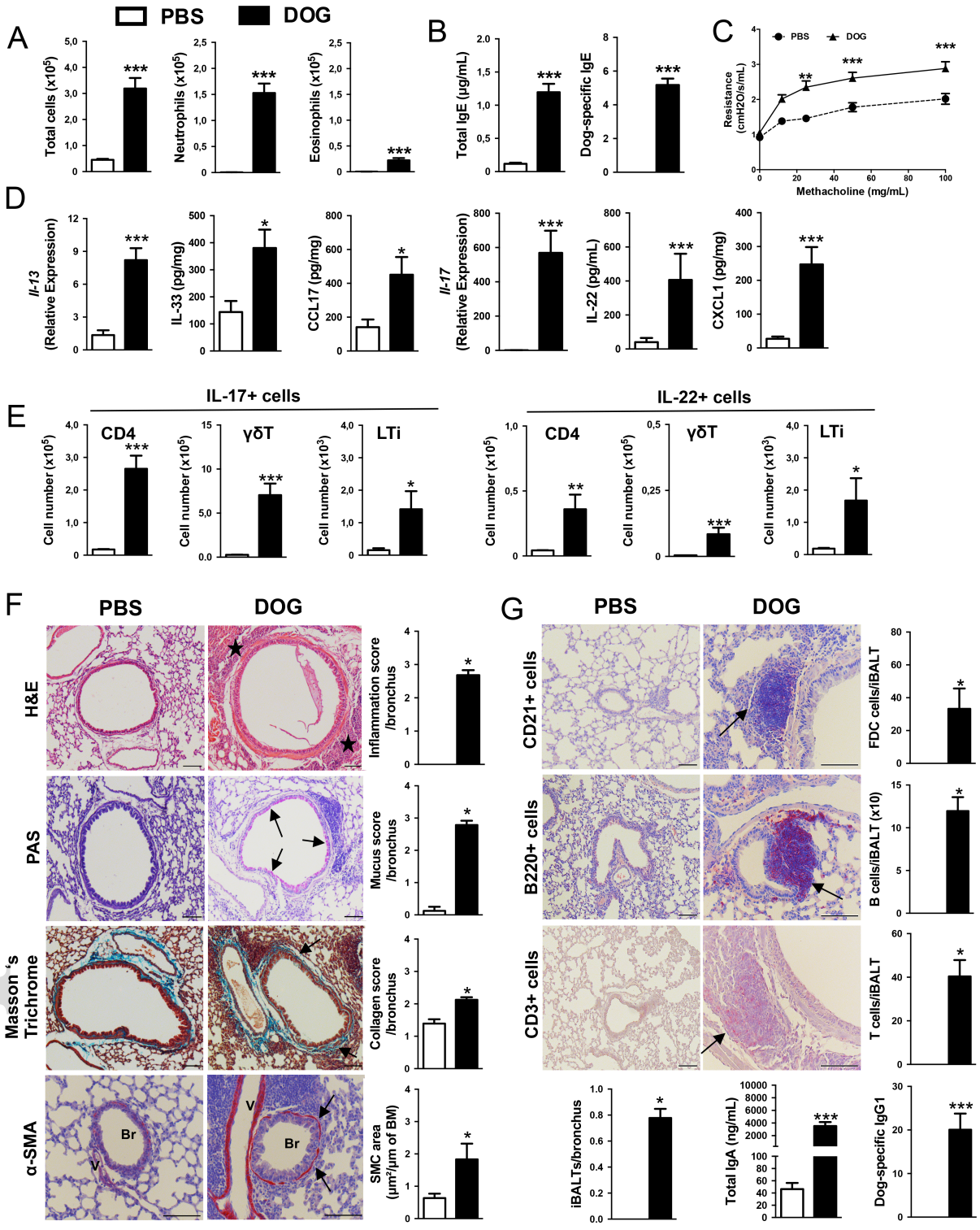
This article is protected by copyright. All rights reserved

A, Human Ahr reporter activity of dog allergen. Mean relative luciferase luminescent unit in response to positive control FICZ, negative control (medium and LPS) and to dog, Can f 1, Can f 2, Can f 3 and HDM allergens. IR: index of reactivity. Data are expressed as mean ± SEM of 2 separate experiments in quadruplicate **B,** BAL absolute number of cells, serum total and specific IgE (titers), AHR. **C,** Lung cytokine production **D,** Quantification of lung sections for inflammation score using H&E, mucus score using PAS, SMC using α-SMA antibody (positive cells are stained in red), BM: basement membrane, **E,** BAL total IgA and dog allergen-specific IgG1. **F,** Representative photographs and/or quantification of iBALT for FDC, B cells and T cells. Positive cells are stained in red, scale bars: 100 µm. Black arrows show staining of interest. Data are presented as mean ± SEM of n mice per group (n=6-14 for B and C; n=4-6 for histology, n=6-8 mice for BAL) *p<0.05, **p<0.01, ***p<0.001, versus control, $^{\#}$p<0.05, $^{\#\#}$p<0.01, $^{\#\#\#}$p<0.001. One-way ANOVA for all, except for the antibody response, SMC, T cells (Kruskal Wallis), and two-way ANOVA for AHR.

Accepted Article

This article is protected by copyright. All rights reserved

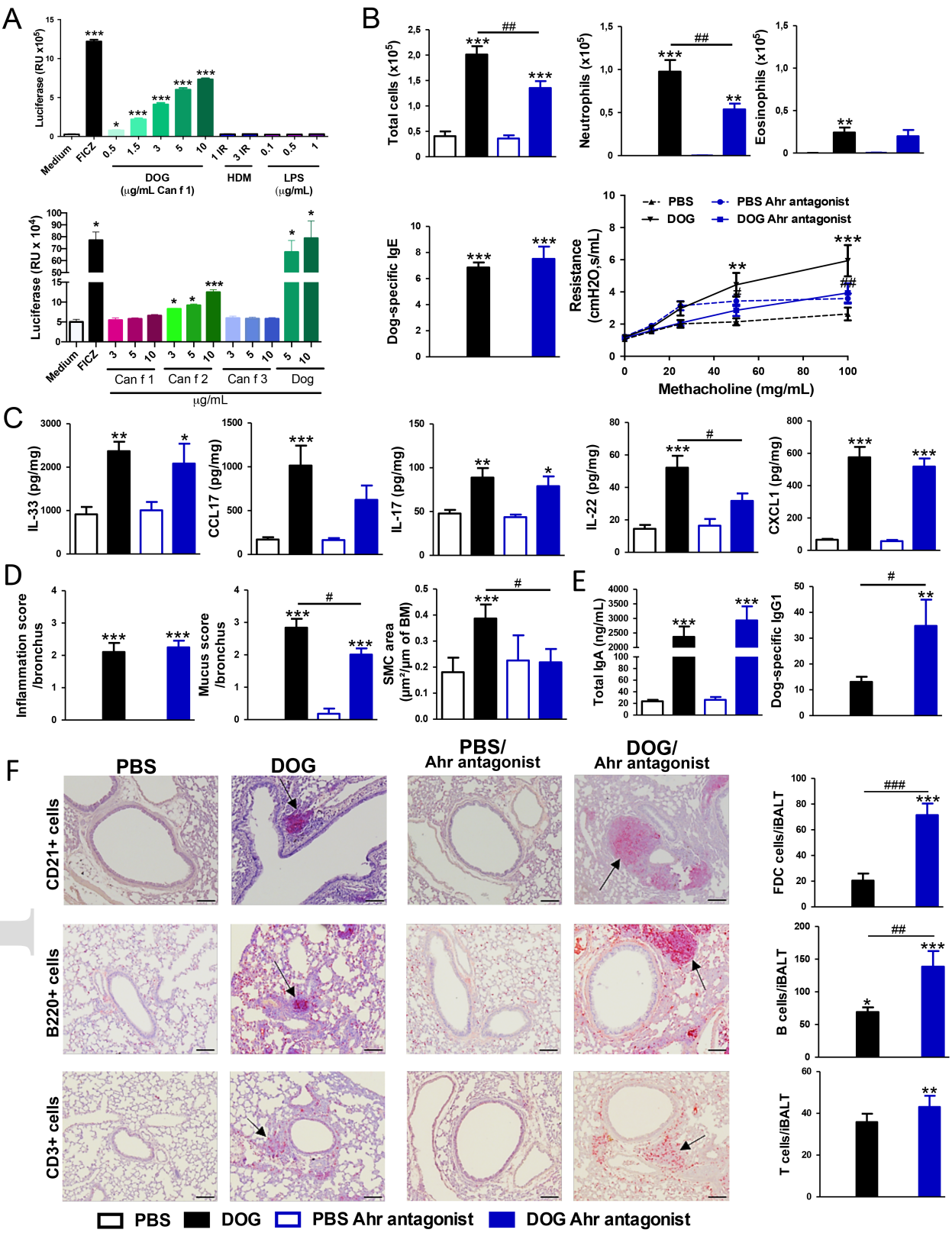
Accepted Article



all_14740_f1.tif

This article is protected by copyright. All rights reserved

Accepted Article



all_14740_f2.tif

This article is protected by copyright. All rights reserved

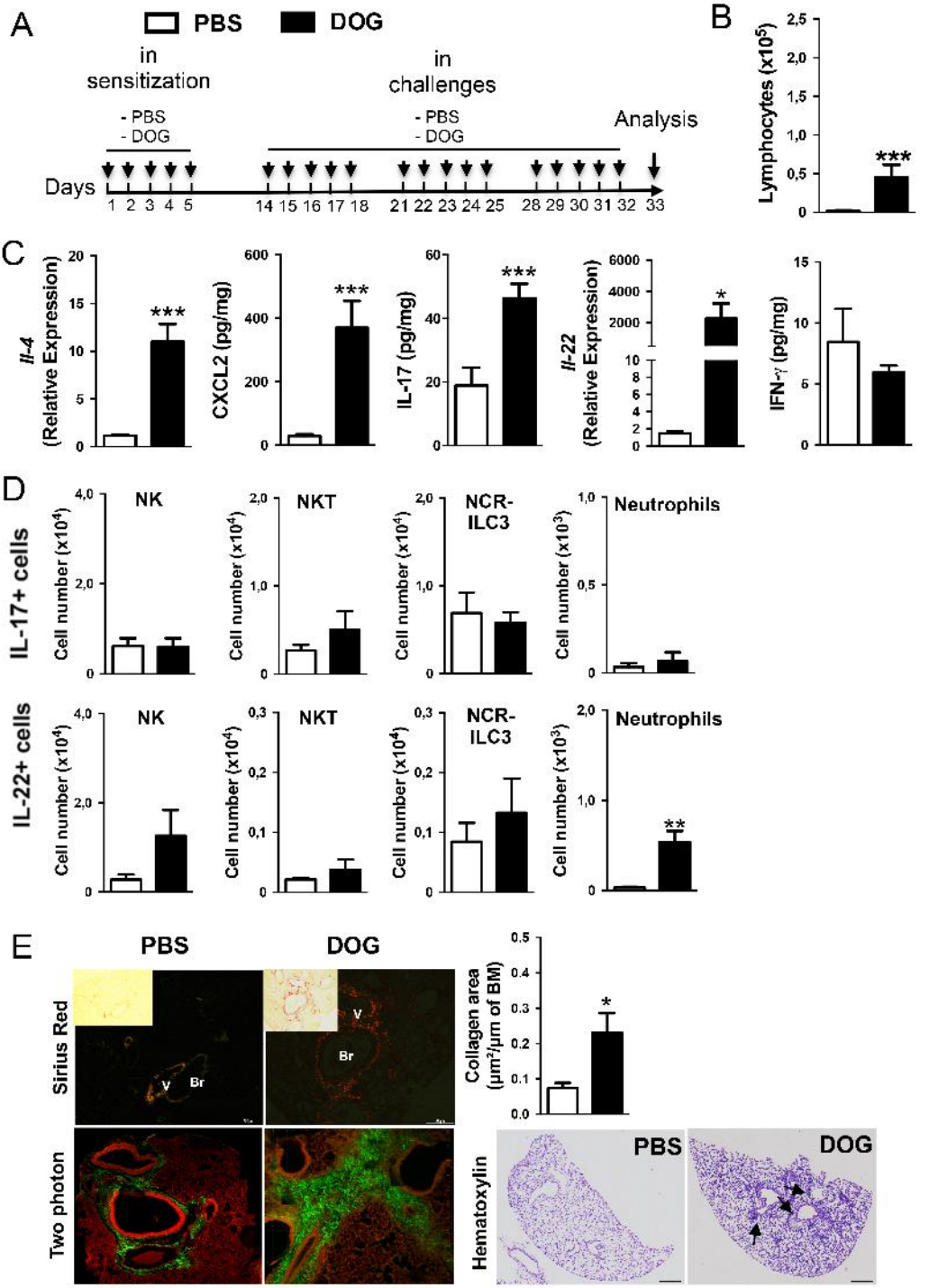


Figure S1. A, Experimental design, i.n.: intranasa.l **B,** BAL absolute number of cells. **C,** Levels of cytokines in lung extracts. **D,** Numbers of IL-17$^+$ and IL-22$^+$ cells in the lungs. **E,** Representative photographs and quantification of stained lung sections for collagen and iBALT. Collagen depots in red assessed by Picrosirius Red Stain (insets correspond to sections under non polarized light). Scale bars: 500 µm. V: vessel, Br: bronchus, BM: basement membrane. Two photon microscopy of lung sections showing collagen in green and lung structures in red. iBALTS structures (black arrows) visualized by hematoxylin staining. Data are presented as mean ± SEM of n mice per group (n=14-32 for B, n=8-20 for C, n=6-15 for D, and n=4-7 for histology). *p<0.05, **p<0.01, ***p<0.001, versus PBS. Mann Whitney test for all.

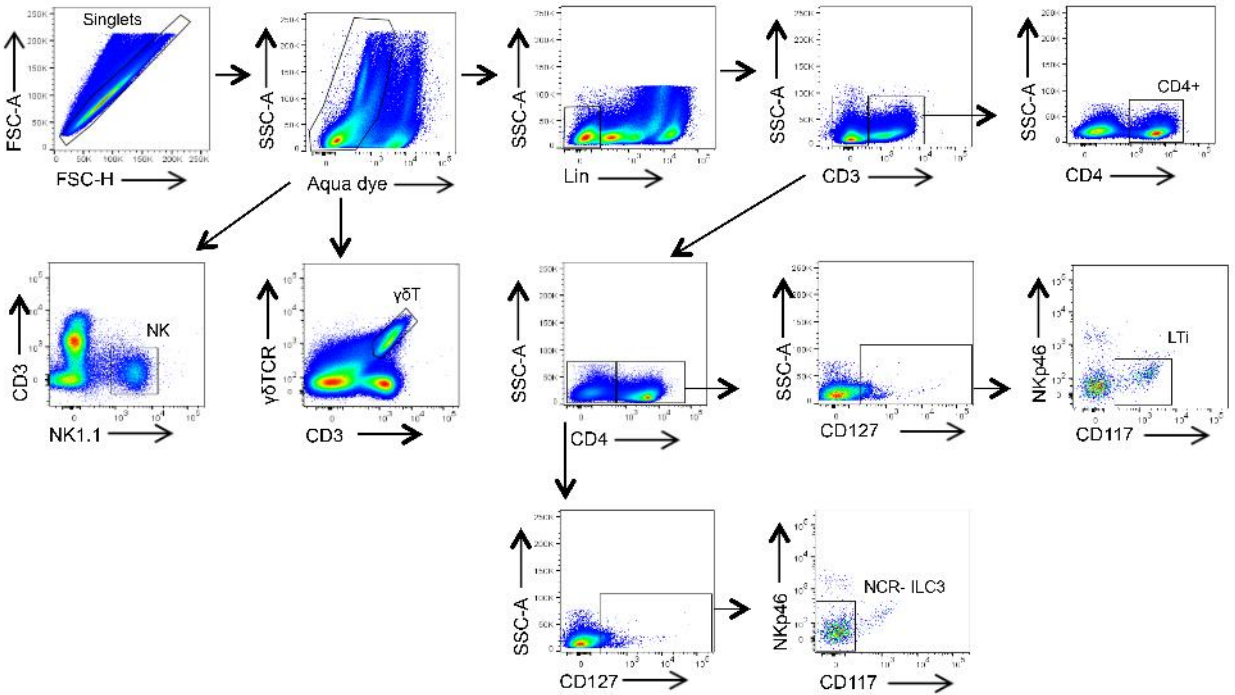


Figure S2. Gating strategy of cell subsets in the lung for NK, γδT, ILC and CD4⁺ cells. LTi: lymphoid tissue inducer cells; NCR: Natural cytotoxic receptor. Gating strategy included forward and side scatter gating, exclusion of multiplets, selection of living cells with live aqua dead, and selection of cell subsets according to the indicated cell surface markers.

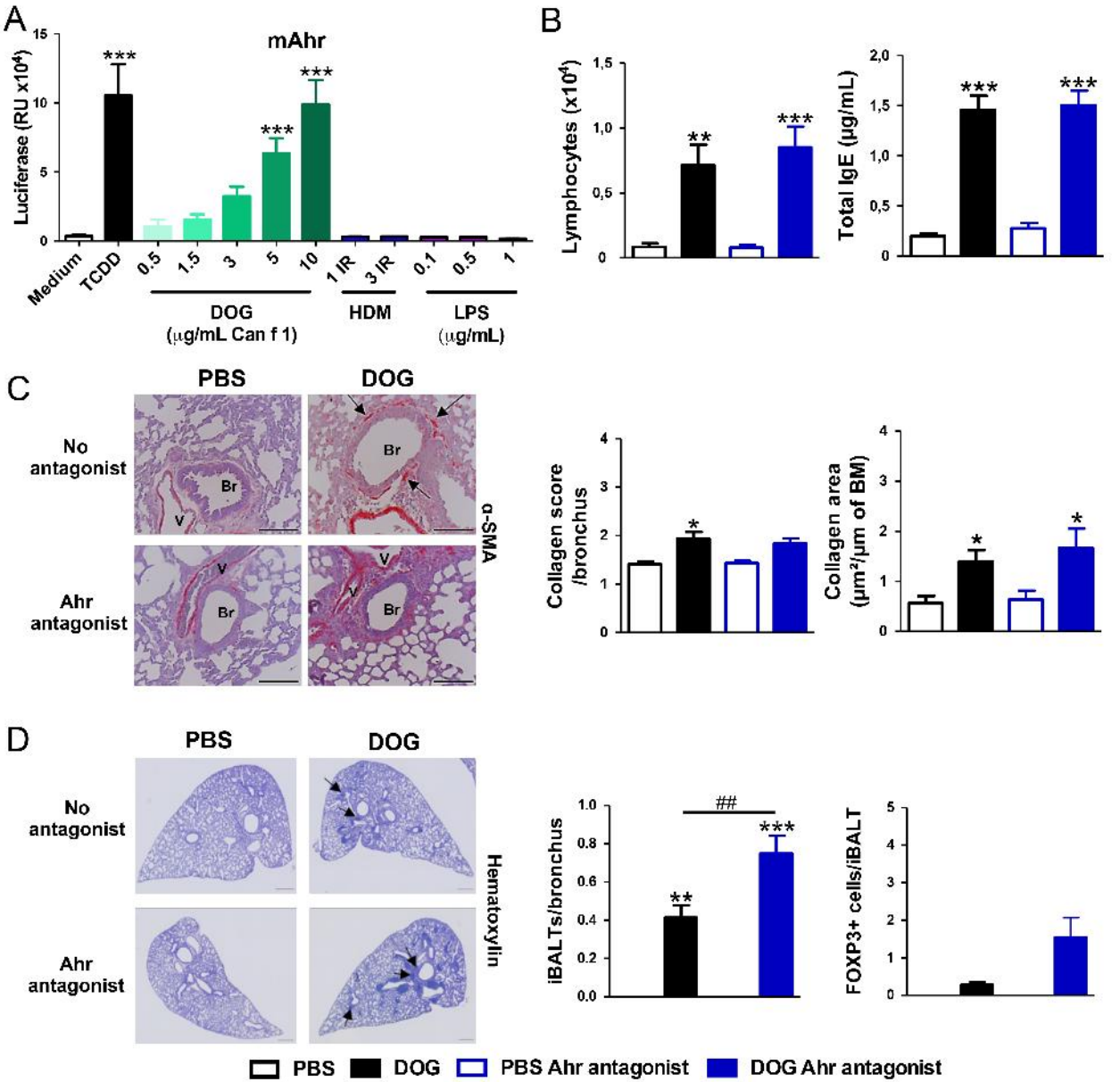


Figure S3. Effects of Ahr antagonist in dog allergen-induced AAI. **A,** Murine Ahr reporter activity of dog allergen. Mean relative luciferase luminescent unit in response to positive control TCDD, negative control (medium and LPS) and to dog and HDM allergens. IR: index of reactivity. Data are expressed as mean ± SEM of 2 separate experiments in quadruplicate. **B,** BAL absolute number of cells and serum total IgE. **C,** Representative photographs of α-SMA staining in lung sections, and quantification of lung sections for collagen score using Masson's trichrome, and collagen area using Picrosirius Red Stain. **D,** Representative photographs and/or quantification of iBALT numbers and of iBALT Foxp3⁺ cells. Positive cells are stained in red, scale bars: 100 µm for C and 500 µm for D. V: vessel, Br: bronchus, Black arrows show staining of interest. BM: basal membrane. Data are presented as mean ± SEM (n=6-14 mice per group; n=4-6 mice per group for histology) *p<0.05, **p<0.01, ***p<0.001, versus control, ##p<0.01. One-way ANOVA for all, except for total IgE (Kruskal Wallis).

Supporting information

Bouté et al: Direct activation of the aryl hydrocarbon receptor by dog allergen participates in neutrophilic airway inflammation

Mice, reagents, allergen sensitization and challenges

C57BL/6J female mice (6 weeks of age) were purchased from Charles River or Janvier Lab (France) and housed under specific pathogen-free conditions. All animal experiments were approved by the regional ethical committee and authorized by the ministry of research and innovation (APAFIS#7874-2016070417344442 v3). The concentration of the major dog allergen Can f 1 in dog allergen extracts was evaluated by ELISA (Indoors biotechnology, Cardiff, UK). For Ahr experiments, the antagonist CH-223191 (Tocris, Noyal Châtillon sur Seiche, France) was administered only during the challenge phase. The amount of Ahr antagonist added to the diet was calculated as previously described[1] and was ~10mg/kg/day, an amount shown to be efficient in blocking Ahr *in vivo*. After having performed dose response experiments, positive groups were sensitized intranasally (i.n.) with dog allergen extract (kindly provided by Stallergenes and ALK France) at a dose corresponding to 10 μg/mL of the major allergen Can f 1 in 30 μL of PBS, or for the control groups with PBS alone for 5 days. Nine days later, mice were challenged i.n. with the same quantity of dog allergen (positive groups) or PBS (control groups) 5 days a week for 3 weeks (Figure S1A). AHR was assessed 24 hours after the last challenge. For Ahr experiments, mice were fed during allergen challenges with either normal control diet alone (D12450K, Research Diet, New Brunswick, USA), or the same diet supplemented with the Ahr antagonist CH-223191 (Tocris, Noyal Châtillon sur Seiche, France). Mice were sacrificed by pentobarbital injection (Euthasol, Centravet). BAL fluid was collected and cells counted on cytospin preparations after May-Grünwald Giemsa (Diapath, Microm Microtech, Brignais, France) staining.

Measurement of serum and BAL antibodies

Total IgE serum level was measured by ELISA as previously described.[2] For dog-specific IgE antibodies, 96-well plates (Corning Incorporated, NY, USA) were coated with 10 μg/mL Can f 1-containing dog allergen in PBS. After blocking with 0.05% tween 5% milk in PBS, and serum or BAL samples addition, an anti-mouse IgE antibody coupled to HRP (GENTAUR, Paris, France) was added in CGS2 Buffer (Can Get Signal for secondary Antibody, Cosmo Bio, Japan), followed by addition of TMB substrate solution (Sigma Aldrich, Saint-Quentin Fallavier France). For dog-specific IgG1 antibodies, 96-well plates were coated with 10 μg/mL Can f 1-containing dog allergen in PBS. After blocking with 3% BSA, and serum or BAL samples addition, an anti-mouse IgG_1 antibody coupled to HRP (Fischer Scientific, Illkirch, France) was added with 0.5% BSA in PBS followed by addition of TMB substrate

solution (Sigma Aldrich). The dog-specific antibody titers of the samples were determined with a pooled standard that was generated in the laboratory. Titers were expressed as the inverse of the dilution corresponding to 50% of the maximal optical density. Total IgA in BAL was assessed using IgA mouse ELISA kit according to the manufacturer's instructions (eBioscience, San Diego, USA).

Measurement of airway responsiveness

AHR was assessed and analysed using Flexivent® (Scireq®, Montreal, Canada) as previously described.[3]

Lung histology and immunohistochemistry

The left unwashed lung from each mouse was fixed in Antigenfix (Microm Microtech, Brignais, France) and embedded in paraffin (Histowax, Microm Microtech) according to the manufacturer's indications. Lung sections of 5 µm were stained with a standard Hematoxylin & Eosin stain (Microm Microtech,) to evaluate peribronchial inflammation. Bronchial cell infiltration was quantified using the following score:[4] 0, no mononuclear cell infiltration; 1, few mononuclear cells; 2, from 1 to 5 layers of inflammatory cells around bronchi; 3, thickness of inflammatory cells > 5 cells and surrounding the entire bronchus. For airway remodelling, mucus production, collagen deposition and smooth muscle cell immunostaining were assessed. For mucus, Periodic Acid-Schiff staining kit (Clinisciences, Nanterre, France) was used for mucopolysaccharide staining. Mucus production in the airway epithelium was quantified based on a five-point system: 0, no mucus; 1, <25% of the epithelium; 2, 25–50% of the epithelium; 3, 50–75% of the epithelium; 4, >75% of the epithelium as previously described.[5] For collagen deposition, sections were stained with Masson's trichrome (Clinisciences) and with Picrosirius Red Stain kit (PolyScience, Niles, USA). Quantification of peri-bronchial collagen deposition by Masson's trichrome was scored as:[6] 1, marginal peri-bronchial trichrome stain; 2, slight increase in peri-bronchial trichrome stain; 3, increased peri-bronchial thickness in trichrome stain; 4, dramatically increased thickness of trichrome stain in all airways. Data were expressed as mean scores per bronchus. Picrosirius red staining was quantified under polarized light (Nikon, SMZ25) using image J software and expressed as surface area µm²/µm of bronchus basement membrane. Collagen was also imaged by two-photon confocal microscopy (Leica Sp8). Thick lung sections (100 µm) were cut and imaged by second harmonic generation that captures triple helical collagen molecules. Smooth muscle cells (SMC) were identified by immunohistochemistry using a primary rabbit anti mouse α-SMA antibody (clone E184, Abcam, Paris, France), the rabbit Vectastain ABC-Alkaline Phosphatase kit (Vector Laboratories, Peterborough, United Kingdom), and developed using fast red (Sigma Aldrich). Quantification was performed in small bronchi using image J software and expressed as μm^2 surface area /µm of bronchus basal membrane. For induced Bronchus Associated Lymphoid Tissue (iBALT) analysis, the

number of iBALT follicles was counted. Data were expressed as number of iBALT per bronchus. BALT B cells, T cells, Foxp3^{+} cells and follicular dendritic cells (FDC) were identified by immunohistochemistry. Sections were incubated with a primary rabbit monoclonal antibody against murine CD21 FDC (Sigma Aldrich, clone EP3093), rat antibody against CD45R B cells (clone RA3-6B2, eBioscience), rabbit antibody against CD3-ε T cells (clone SP7, Abcam) and rat anti-mouse Foxp3 (clone FJK-16s, eBioscience) after a step of antigen retrieval. The corresponding Vectastain ABC-AP kit was then used and the colour developed using Fast Red substrate kit (Sigma Aldrich). Numbers of positive cells were enumerated using an ocular grid and expressed as number of positive cells per iBALT. All data measurements were performed in 3 to 9 different lung sections and averaged for each mouse. Quantification was performed blindly in whole lung sections.

Gene expression analysis

mRNA levels were assessed by RT-qPCR. Lung tissue RNA samples were isolated using NucleoSpin RNA (Macherey Nagel, Hoerdt, France). Extracted RNA was reverse-transcribed with the High-Capacity cDNA reverse transcription kit (Applied Biosystems, USA), according to the manufacturer's instructions. The resulting cDNA was amplified using the IDT Prime Time Assay master mix. Real Time-PCR was performed with Prime Time Assay primers (IDT, Leuven, Belgium). They were detected on a QuantStudio 3 (Applied Biosystems, Waltham, USA). Data were analysed via the Thermo Fisher cloud. *Rplp0* (Ribosomal Protein Lateral Stalk Subunit P0) was used as internal reference gene to normalize the transcript levels. Relative mRNA level ($2^{-\Delta\Delta Ct}$) was determined by comparing the PCR cycle thresholds (Ct) for the gene of interest and internal reference gene (ΔCt) and ΔCt values for treated and control groups ($\Delta\Delta$Ct).

Quantification of chemokine and cytokine levels

Lung protein extracts were prepared after mechanical dissociation of one lung lobe in 1 mL of lysis buffer (Tissue-Protein Extraction Reagents, Life Technologies, Villebon-sur-Yvette, France) and protease inhibitor cocktail (Sigma Aldrich) at +4°C. Supernatants were collected for further total protein (Pierce BCA proteins Assay kit, Life technologies), cytokine and chemokine measurements. The levels of IL-33, IL-17, IL-22, IFN-γ cytokines, and CCL17, CXCL1 chemokines were assessed using commercial ELISA kits (detection limit 25, 15.6, 23, 31.2, 31.2 and 63 pg/mL respectively) according to the instructions provided by the manufacturers (eBioscience, Peprotech (Neuilly-Sur-Seine, France) and R&D Systems (Abingdon, UK)). Data are expressed as pg per mg of total proteins, or per mL for BAL fluid measurements.

Flow cytometry analysis

For flow cytometry, lungs were perfused through the pulmonary artery and digested in 1 mg/mL type IV collagenase (Gibco, Life Technologies) and 2 IU/mL DNase I (Roche

Diagnostics, France) in RPMI 1640 (Dutscher, France) for 30 minutes at 37°C. Cells were collected, filtered on a 70 µm-pore membrane, and centrifuged at 670 x g during 15 minutes on a Percoll density gradient (GE Heathcare, Chicago, USA). Erythrocytes were lysed in Red Blood Cell Lysis Buffer (Biolegend, London, UK). Cell suspensions were stimulated for 2 hours at 37°C with 10 ng/mL phorbol 12-myristate 13-acetate (Invivogen), 0.5 µg/mL ionomycin (InvivoGen, Toulouse, France) and brefeldin (eBioscience). Cells were then treated with Fc Block (anti-CD16/CD32 antibody, BD-Biosciences). For cell surface staining, specific antibodies or corresponding control isotypes were added for 20 minutes. NK, NKT, γδ cells were stained using CD3-AF700, NK1.1-BV786, CD1d-tetramer-PE, TCRβ-BV605, γδTCR-PE-Cy7, and defined as $CD3^-NK1.1^+$, $TCR\beta^+CD1d\text{-}tetramers^+$ and $CD3^+TCR\gamma\delta^+$ respectively. Macrophages and neutrophils were stained with CD11c-PE-CF594, CD11b-PerCP-Cy5.5, F4/80-BV650, Ly6G-BV711, and defined as $CD11c^+F4/80^+CD11b^+$, and $CD11c^-CD11b^+Ly6G^+F4/80^-$ respectively. For T cells and Innate lymphoid cells (ILC) $Lineage^-$ cells (Lin^-) were gated out by the use of FITC- conjugated antibodies to CD11b, CD19, FcεRI, TER-119, Ly6G (GR-1), CD49b (DX5), CD11c, F4/80, TCRγδ, preceded by a $CD45^+$ cell selection with a CD45 APC-Cy7. The lymphoid populations of interest were selected using NKp46 PerCP-eFluor710, CD117 BV650, CD3 Alexa Fluor 700, CD127 BV786, CD4 BV605, and defined as CD4+: Lin-CD3+CD4+; ILC3NCR$^+$: $Lin^-CD3^-CD4^-CD127^+CD117^+NKP46^+$; ILC3NCR$^-$: $Lin^-CD3^-CD4^-CD127^+CD117^{low}NKP46^-$; LTi: $Lin^-CD3^-CD4^+CD127^+CD117^+NKP46^-$. All these antibodies were from eBioscience and BD, except TCRγδ from Invitrogen). Cells were fixed and permeabilized using the BD Cytofix/Cytoperm kit and stained intra-cellularly with antibodies directed against IL-22-APC or -PE and IL-17-BV421 or the corresponding FMO or control isotypes. PBS-57-loaded CD1d tetramers were obtained from the NIAID (National Institutes of Health) Tetramer Facility (Emory University, Atlanta, GA). The monoclonal Ab against mouse IL-22 (clone 3F11) and its control isotype were a kind gift from Dr. W. Ouyang (Genentech, San Francisco, CA), and were labelled with the APC or PE conjugation kit from AbD Serotec (Colmar, France). Cell fluorescence was measured by flow cytometry (LSR FORTESSA®, BD Biosciences) and analysed using the Flow Jo v10.6.1. software. The percentage of cytokine positive cells is shown after subtraction of the corresponding isotype control. The gating strategy is presented in Figure S2.

Ahr reporter assays

The HepG2-Lucia™ Ahr cells (InvivoGen) express endogenous Ahr and stably express the secreted Lucia luciferase reporter gene under the control of a promoter coupled with the human *Cyp1a1*. Cells were handled according to the manufacturer's instructions. Briefly, cells were seeded in 96-well plates at $2x10^4$ cells per well and stimulated with formylindolo[3,2-b]carbazole (FICZ) at 1 µg/mL or 2,3,7,8-tétrachlorodibenzo-p-dioxine

(TCDD) at 0.01 □M as a positive control, with LPS as negative control, and with dog, Can f 1, Can f 2, Can f 3 or House dust mite allergen (Stallergenes/Greer) for 48 hours. Supernatants were collected and QUANTI-Luc™ (InvivoGen) added just before luminometer measurement. A second reporter cell line, the H1L7.5c3 mouse hepatoma, kindly provided by Michael Denison was also evaluated. Cells were seeded at $7.5x10^4$ cells per well for 24 hours and then stimulated with the above reagents for 12 hours and handled as previously described[7]. The results are expressed as relative luciferase units.

Statistical analysis

When more than two groups were compared, normally distributed data (Shapiro-Wilk normality test) were analysed by one-way analysis of variance (ANOVA), followed by post-hoc multiple comparison test (Bonferroni test). Non-normally distributed data were analysed by the Kruskal-Wallis test followed by Dunn's multiple comparison test. When two groups were compared, the Mann Whitney test was used. For AHR a two-way ANOVA test was used. The Graphpad prism v8 software was used. p values <0.05 were considered statistically significant.

References

1. Dean A, Gregorc T, Docherty CK, Harvey KY, Nilsen M, Morrell NW, et al. Role of the Aryl Hydrocarbon Receptor in Sugen 5416-induced Experimental Pulmonary Hypertension. Am J Respir Cell Mol Biol. 2018;58:320-30.
2. Ait Yahia S, Azzaoui I, Everaere L, et al. CCL17 production by dendritic cells is required for NOD1-mediated exacerbation of allergic asthma. *Am J Respir Crit Care Med*. 2014;189:899-908.
3. Everaere L, Ait-Yahia S, Molendi-Coste O, et al. Innate lymphoid cells contribute to allergic airway disease exacerbation by obesity. *J Allergy Clin Immunol*. 2016;138:1309-18 e11.
4. Paulissen G, Rocks N, Gueders MM, Bedoret D, Crahay C, Quesada-Calvo F, et al. ADAM-8, a metalloproteinase, drives acute allergen-induced airway inflammation. Eur J Immunol. 2011;41:380-91.
5. Myou S, Leff AR, Myo S, Boetticher E, Tong J, Meliton AY, et al. Blockade of inflammation and airway hyperresponsiveness in immune-sensitized mice by dominant-negative phosphoinositide 3-kinase-TAT. J Exp Med. 2003;198:1573-82.
6. Le Saux O, Teeters K, Miyasato S, Choi J, Nakamatsu G, Richardson JA, et al. The role of caveolin-1 in pulmonary matrix remodeling and mechanical properties. Am J Physiol Lung Cell Mol Physiol. 2008;295:L1007-17.
7. He G, Tsutsumi T, Zhao B, Baston DS, Zhao J, Heath-Pagliuso S, et al. Third-generation Ah receptor-responsive luciferase reporter plasmids: amplification of dioxin-responsive elements dramatically increases CALUX bioassay sensitivity and responsiveness. Toxicol Sci. 2011;123:511-22.